Rare Metal Materials and Engineering
Volume 54, Issue 9, September 2025
Available online at www.rmme.ac.cn

Science Press

Cite this article as: Jiang Zhongyu, Xu Guangming. Effect of Different Heat Treatments on Surface Microstructures and Anodic Oxide Film Structures of Al-5.6Mg Alloy Sheets[J]. Rare Metal Materials and Engineering, 2025, 54(09): 2205-2210. DOI: https://doi.org/10.12442/j.issn.1002-185X.20240492.

ARTICLE

Effect of Different Heat Treatments on Surface Microstructures and Anodic Oxide Film Structures of Al-5.6Mg Alloy Sheets

Jiang Zhongyu, Xu Guangming

Key Laboratory of Electromagnetic Processing of Materials, Ministry of Education, Northeastern University, Shenyan 110819, China

Abstract: The effect of different intermediate annealing heat treatments on the surface microstructures and anodic oxide film structures of rolled Al-5.6Mg sheets was studied. The results show that when the continuous annealing is used to control microstructures of the sheets instead of the static state annealing in the intermediate annealing process, the surface grain size of the sheets can be reduced by about 65.7%, and the size of the Mg precipitation phase (Mg_2Al_3) can be reduced by about 67%. Under the combined influence of grain size, precipitation phase, and texture, the highest glossiness can be obtained, which is attributed to continuous intermediate annealing and stabilization annealing at low temperature. The uniform grain and precipitation structures is beneficial to reducing the inhomogeneous dissolution of the oxide film and to obtain the anodic oxide film with uniform thickness and high glossiness.

Key words: heat treatment; anodizing; Al-Mg alloy; microstructures

1 Introduction

Sheets of AA5xxx aluminum alloys are widely applied to computer, communication, and consumer electronics (3C) industries because of their beautiful appearance surface and tinctorial diversity after anodizing, as well as high surface hardness and lightweight[1]. However, in recent years, with the growing demand for lightweight, convenient, and aesthetically appealing aluminum products, there has been a greater focus on performance such as higher strength, excellent surface glossiness, and greater cost-effectiveness.

Many 5xxx aluminum alloys, especially the ones with high Mg content such as AA5182 and AA5059, have low or poor external glossiness after anodizing. This has become a significant reason in the efforts to improve and control the appearance quality of high-Mg-content aluminum alloys in the aluminum industry. This is why the 5xxx aluminum alloy is a hot topic for research and development currently.

In the existing literatures, researchers studied the effects of chemical composition of the 5xxx aluminum alloys and anodizing process parameters on the appearance quality after anodizing[2–7]. Ding et al[8] also investigated the corrosion rate of the secondary phase during anodizing. Additionally, Asahina et al[9] found that single crystal with different crystal orientations after anodizing has different surface performances. Kato[10] observed that the reflectivity of the oxide film obtained after anodizing on different crystal planes was different.

However, there are few studies on the effect of heat treatment processes on the microstructures and anodic oxide film structures of 5xxx aluminum alloys with high Mg content. There are two main types of heat treatment: static state annealing and continuous annealing. Continuous annealing generally produces a fine-grained and high-strength aluminum alloy with uniform properties. To increase efficiency of production, continuous annealing is frequently used in aluminum industries[11]. With the growing application of aluminum sheets, continuous annealing production line is now widely used for various aluminum alloy products to improve the properties of aluminum alloy sheets, and the number of that has rapidly increased[12–14].

In this study, the Al-5.6Mg alloy was studied and

Received date: October 07, 2024
Corresponding author: Jiang Zhongyu, Master, Professor, Key Laboratory of Electromagnetic Processing of Materials, Ministry of Education, Northeastern University, Shenyan 110819, P. R. China, E-mail: zhy_jiang@chinalco.com.cn

developed. The effects of different heat treatments during intermediate annealing, including static state annealing and continuous annealing, on the final microstructures, surface crystallization texture, and structures of oxide film after anodizing were analyzed. The relationship among heat treatment, microstructures of Al-5.6Mg alloy sheets, and performance of surface anodic oxide film was established. The findings from the observations and analysis in this work provided a guidance and an improving direction for heat treatment processing of the high-Mg-content 5xxx aluminum alloy sheets with high strength and high glossiness after anodic oxidation.

2 Experiment

The composition of the Al-5.6Mg alloy was designed and listed, as shown in Table 1. The composition of the aluminum alloy is in accordance with AA5023 alloy certification. It contains a very high mass percentage of Mg, while the mass percentages of other elements are kept at very low levels. A large ingot with commercial size of the Al-5.6Mg alloy was produced using high purity aluminum as raw material. The final composition of the ingot met the design requirements of the Al-5.6Mg alloy, as listed in Table 1.

A sheet with the thickness of 3.7 mm was obtained through conventional hot rolling process. To achieve full recrystallized grain structure, the final hot rolling temperature was set at 320 °C. The hot rolled sheet was then cold rolled by four passes to 1.0 mm in thickness, as shown in Table 2.

After the above cold rolling, intermediate annealing was conducted. Static state annealing and continuous annealing were performed in a box furnace and a continuous annealing furnace on industrial scale, respectively. The two annealing schedules are designed to obtain full recrystallization structures.

The static state annealing was held at 330 °C for 2 h, followed by cold rolling to achieve the final thickness of 0.8 mm. Stabilizing annealing was then performed at 100 °C and 200 °C for 2 h, resulting in sample 1# and 2#, respectively.

For continuous annealing, the goals were to obtain recrystallized sheet and to control size and number of precipitated phase particles. Taking industrial factors into account, continuous annealing was conducted at 380 °C for 15 s, followed by the same cold rolling to achieve the thickness of 0.8 mm and stabilizing anneal processing at 100 °C and 200 °C for 2 h, resulting in sample 3# and 4#, respectively.

Grain structures and compound phase particles were observed by the optical microscope (OM), and oxide film was examined by a scanning electronic microscope (SEM, EVO MA10). The grain size was measured using an optical method in accordance with ASTM E112-13 standard. Electron backscattered diffraction (EBSD) measurement and analysis were conducted by SEM (JSM 7800F) and Oxford software with advanced analysis capabilities. Surface roughness was measured with a roughness meter (TIME-3202) and the glossiness was determined by a glossiness meter (KSJ-MG268-F2). Two parameters, R_a and R_z, of surface roughness were measured with a roughness meter (TIME-3202). R_a is the arithmetic mean of the absolute values of the profile deviations from the mean line. R_z is maximum height of the profile.

3 Results and Discussion

Fig. 1 shows the surface grain structures and the surface feature of Mg-containing phase of four samples after direct corrosion by phosphoric acid solution. By comparing Fig. 1a–1d, it can be observed that the two annealing processes lead to different grain sizes. The grain sizes of the samples 1# and 2# from the static state annealing are obviously larger than those of the samples 3# and 4# from the continuous annealing. The grain size measurement shows that the continuous annealing results in a grain size of about 12 μm, whereas the static state annealing results in a grain size of about 35 μm. Continous annealing can reduce the surface grain size by 65.7% compared to static annealing. The findings of Samberger[15] and Cheng[16] et al indicated that the rapid annealing leads to smaller grain sizes after cold deformation, which is also reflected in the industrial results, as shown in Fig. 1a–1d.

According to the study from Zhao et al[17], the size and quantity of Fe-containing phase do not change during cold rolling and annealing, so the Fe-containing phase will not be considered here because of the low mass percentage of Fe (Table 1). Yang et al[18] noted that in 5xxx series aluminum alloys with Mg>3.5wt%, the Mg-containing phase (Mg_2Al_3) precipitates along the grain boundary during heat treatment. Popović et al[19] proposed that the Mg-containing phases along the grain boundaries of 5xxx series aluminum alloy can be directly corroded by a phosphoric acid solution with a concentration of 10vol% at 60 °C. Following the corrosion method, the Mg-containing phases are directly corroded, as shown in Fig. 1e–1g. It is found that the precipitates are larger

Table 1 Chemical compositions of different alloys (wt%)

Alloy	Si	Fe	Cu	Mn	Mg	Cr	Zn	Al
AA5023	≤0.25	≤0.40	0.20–0.50	≤0.2	5.0–6.2	≤0.10	≤0.25	Bal.
Al-5.6Mg	≤0.10	≤0.12	≤0.10	≤0.2	5.0–6.0	≤0.05	≤0.05	Bal.
Al-5.6Mg Ingot	0.04	0.08	0.02	0.2	5.56	0.03	0.02	Bal.

Table 2 Thickness of sheet after different cold rolling passes

Pass	Thickness/mm
1	2.5
2	1.8
3	1.3
4	1.0

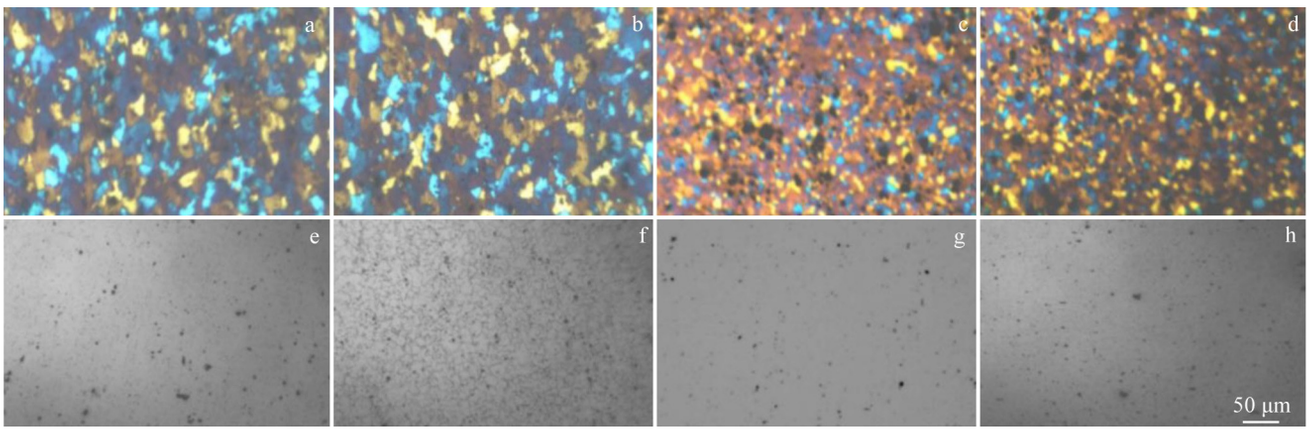

Fig.1 Surface grain structures (a–d) and secondary phase particles after directional corrosion (e–f) of different samples: (a, e) 1#; (b, f) 2#; (c, g) 3#; (d, h) 4#

and more numerous after the static state annealing compared to those after continuous annealing.

Compared to Fig.1e and 1g, it can be observed that the size of the corrosion pits of sample 1# reaches 15 μm after static annealing, which is three times larger than that of sample 3# after continuous annealing. This indicates that the size of the precipitation of Mg-containing phase can be reduced by about 67% after continuous annealing. In addition, it is found that when other process conditions remain unchanged and only the stabilization annealing temperature is increased from 100 °C to 200 °C, the grain size on the surface does not change, but the size and number of corrosion pits increase rapidly and the precipitates grow up.

The main reason for the observed difference is the various heating rates during the continuous and static state annealing processes. In general, the heating rate in continuous annealing exceeds 6 °C/s in industrial scale, which is about 300–600 times faster than that in static state annealing[20]. Due to the rapid heating, more nucleation sites form uniformly in the sheets, resulting in small grain sizes. Additionally, the cooling rate in continuous annealing in this study is fast (close to 10 °C/s), which restricts the grain growth.

At the same time, the rapid cooling also effectively inhibits the precipitation of Mg phase. The finer grain size and the distribution of Al_2Mg_3 phase precipitated in the intermediate continuous annealing are maintained even after stabilized annealing.

Table 3 lists the performance results of the oxide film of the samples after anodization. As shown in Table 3, the surface roughness of the samples after static state annealing is higher, and the glossiness is poorer compared to samples after continuous annealing. Furthermore, increasing the stabilization annealing temperature from 100 °C to 200 °C can reduce the glossiness. The higher the stabilizing annealing temperature, the poorer the surface glossiness.

Table 3 Performance results of anodic oxide film on different samples

Sample	1#	2#	3#	4#
R_a/μm	0.462	0.541	0.454	0.457
R_z/μm	3.483	4.421	3.166	3.262
Glossiness/GU	28	24	48	27

The surface and profile morphologies of the oxide film of samples 2# and 3# with the lowest and highest glossiness, are shown in Fig.2. The uneven features of the oxide film surface in Fig. 2a are significantly different from the local pits , compared to Fig. 2b. A comparison between Fig. 2c and 2d reveals that the thickness of oxide film of sample 2# after static state annealing is 11 μm, which is about 50% of the thickness of sample 3# (20 μm) after continuous annealing.

In general, the growth of the anodic oxide film on aluminum alloys is accompanied by the interfacial reactions between the oxide film and the aluminum matrix, as well as the electrochemical dissolution of the oxide film formed on the surface. Dissolution first occurs at the grain boundary of aluminum alloy. Zhang et al[21] suggested that larger grain sizes can lead to more uneven dissolution of the oxide film during the process of anodization, resulting in a thinner oxide film. Due to the combined influence of more precipitated phase particles and larger grain sizes, the oxide film of the sample 2# undergoes uneven dissolution, leading to an uneven surface feature with reduced thickness. The uneven surface structure results in weaker reflection of incident light and lower glossiness. It has been confirmed that a thick oxide film can achieve high surface glossiness and better protect surfaces of aluminum alloys.

Asahina et al[9] demonstrated that the oxide films on aluminum single crystal with (111), (110), and (100) orientations were formed in a two-step anodization process. It was found that the best ordering was obtained in nanoporous alumina on (100) lattice plane of aluminum single crystal compared to (111) and (110) lattice planes. This indicates that the glossiness after anodization is relative to surface crystal orientations of aluminum sheets.

Fig. 3 and Fig. 4 show EBSD results on the surfaces and volume fractions of different texture components of sample 2# and 3#, respectively. Different crystal orientations are listed in

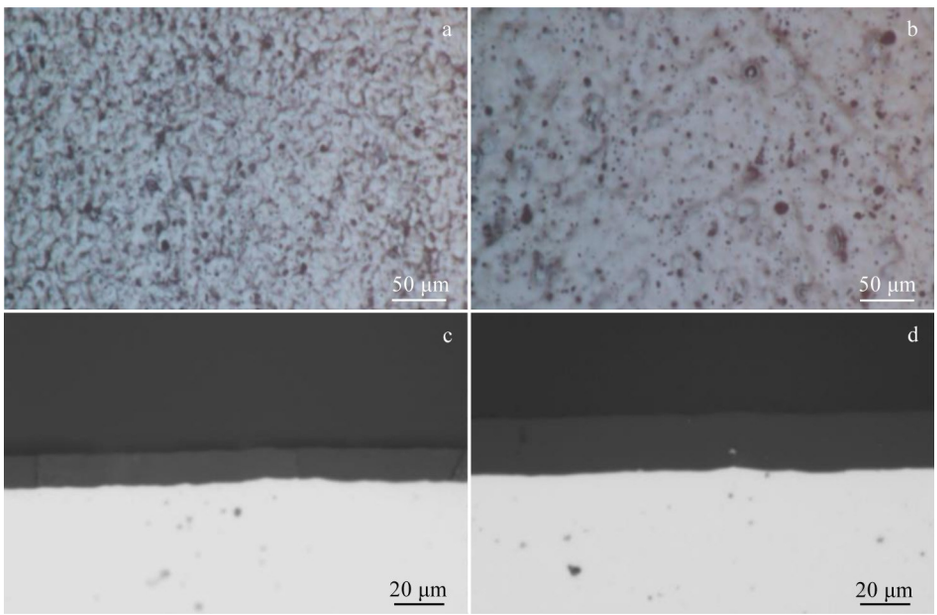

Fig.2 Surface (a–b) and cross-sectional (c–d) morphologies of anodic oxide film of samples 2# (a, c) and 3# (b, d)

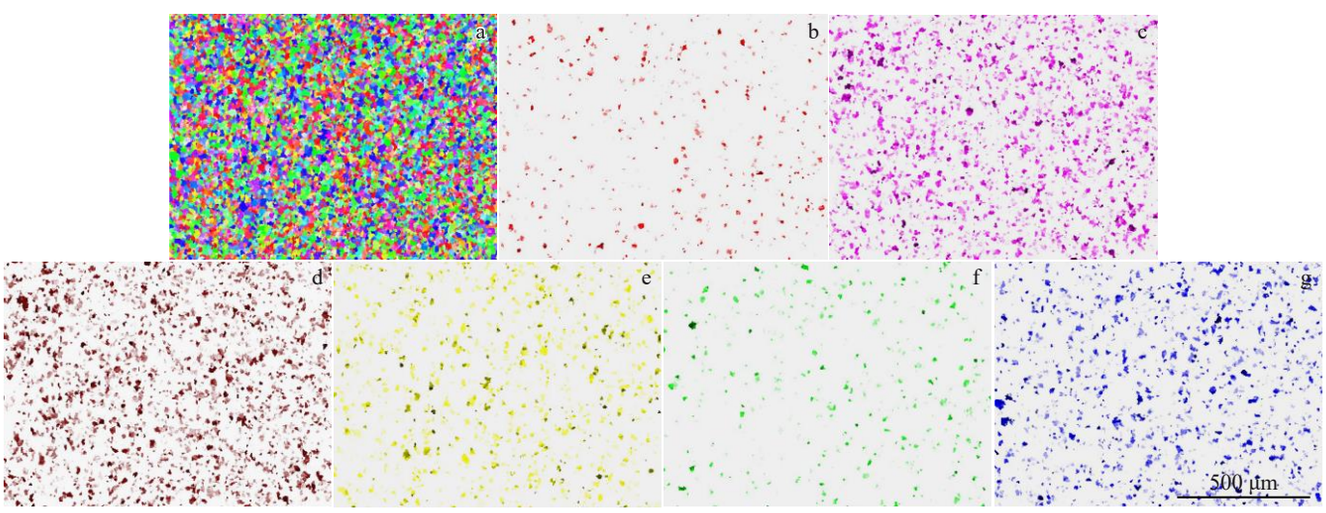

Fig.3 EBSD results of surface of sample 2#: (a) orientation distribution; (b) Cube texture; (c) S texture; (d) R texture; (e) Brass texture; (f) Goss texture; (g) Copper texture

Table 4. In general, the surfaces of aluminum alloy sheets are dominated by deformation textures, including residual deformation texture such as Brass {011}<211>, Copper {112}<111>, and Goss {011}<100>, and recrystallization textures such as Cube {001}<100> and *R* {124}<211>. Sometimes, Goss texture is classified as a recrystallization texture. Grain size analysis results from EBSD are consistent with the optical observation in Fig. 1, further indicating that continuous intermediate annealing reduces grain size.

In addition, based on EBSD analysis from Fig.3–Fig.4, it is found that the Cube texture is uniformly distributed on the surface. The deformation textures are located near and around the Cube texture components. Continuous annealing can produce more grains with Cube orientation compared to static state annealing. According to the study by Asahina et al[9], a high proportion of Cube grains can result in higher surface glossiness. As shown in Table 4, sample 3# has more Cube texture than sample 2#, which corresponds to the higher glossiness of sample 3#. This indicates that a high-volume fraction of Cube components may lead to good surface performance after anodization.

The growth of anodized film along thickness direction on aluminum alloy is accompanied by the formation of oxide film on interface between the aluminum matrix and the electrochemical dissolution of the oxide film on the surface. Zhang et al[21] believed that a larger grain size leads to the more uneven dissolution of the oxide film during the anodizing process, making it easier to achieve a thinner oxide film. This indicated that the dissolution of the oxide film also depends on the crystal orientations. Specifically, grains with

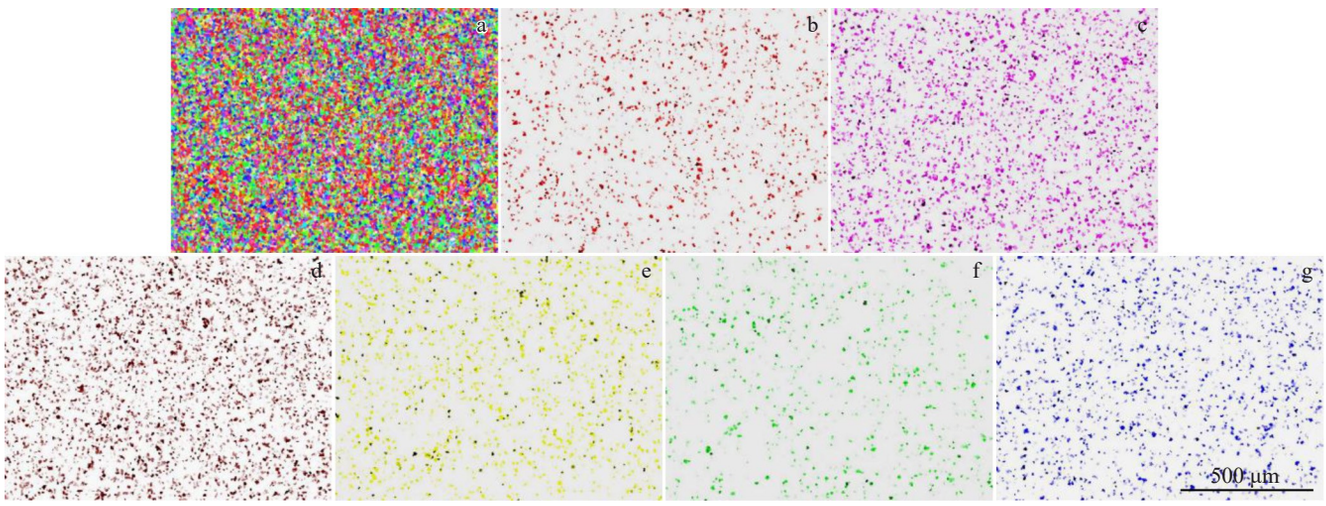

Fig.4 EBSD results of surface of sample 3#: (a) orientation distribution; (b) Cube texture; (c) S texture; (d) R texture; (e) Brass texture; (f) Goss texture; (g) Copper texture

Table 4 Volume fractions of six typical texture components (vol%)

Sample	2#	3#
Copper {112}<111>	12.50	8.38
S {123}<634>	21.40	15.20
Brass {110}<112>	11.20	7.55
Goss {011}<100>	3.46	3.87
Cube {100}<001>	3.40	6.87
R {124}<211>	23.80	18.80

Cube texture may dissolve more slowly compared to other crystal orientations.

Therefore, because of the dual influence of a greater number of precipitated phases and larger grain size, the oxide film of sample 2# is more uneven in the growth and electrochemical dissolution process, resulting in an uneven surface and thinner oxide layers. By studying the impact of grain orientation on anodized oxide film in single crystal, Kato[10] concluded that the reflectivity of the oxide film varies with lattice planes, and the {001} crystal surface has the highest reflectivity compared to the other lattice surfaces.

After examining the anodized film formation process of aluminum alloy, Asahina et al[9] proposed that the oxide film on the {001} crystal plane has the highest reflectivity. In this study, under condition of a larger volume fraction of Cube texture, sample 3# obtains the highest reflectivity of the oxide film, thereby further enhancing the glossiness of the aluminum alloy. The highest glossiness of sample 3# is attributed to the combined effects of grain size, precipitation phase, and texture, as well as the continuous intermediate annealing and stabilization annealing at 100 °C.

4 Conclusions

1) For high-Mg-content 5xxx series aluminum alloy sheets, continuous annealing can reduce the surface grain size by 65.7%, achieving a finer grain size of 12 μm compared to static annealing. Additionally, continuous annealing results in more grains with Cube orientation, which positively influences the properties of material.

2) Continuous annealing significantly decreases the precipitation of Mg-containing phase (Mg_2Al_3) along the grain boundaries by about 67%. These precipitates are uniformly distributed within the grains in sheets processed via continuous annealing.

3) The combination of smaller grain size, uniform precipitation phases, and Cube texture leads to the highest surface glossiness, attributed to continuous intermediate annealing and subsequent low-temperature stabilization annealing. The uniform grain structure with Cube orientation and evenly distributed precipitates help to reduce inhomogeneous dissolution of the oxide film. This enhances the uniformity and glossiness of the anodic oxide film, resulting in a thicker, more consistent film on the aluminum sheets.

References

1 Kong Dejun, Wang jinchun, Liu Hao. *Rare Metal Materials and Engineering*[J], 2016, 45(5): 1122

2 Ma Ke, Jiang Xingxu, Yang Sheng *et al*. *Material Protection*[J], 2023, 56(6): 137 (in Chinese)

3 Lin Shipeng, Ma Ke, Gao Chong. *Light Alloy Fabrication Technology*[J], 2022, 50(4): 31 (in Chinese)

4 Gao Chong, Jiang Zhongyu, Zhao Pizhi *et al*. *Electroplating & Pollution Control*[J], 2020, 40(3): 63 (in Chinese)

5 Gao Wen, Gao Chong, Liu Cheng *et al*. *Aluminum Fabrication*[J], 2021(1): 27

6 Jiang Zhongyu. *Light Alloy Fabrication Technology*[J], 2023, 51(2): 50 (in Chinese)

7 Wu Chunjiang. *Aluminum Fabrication*[J], 2021(5): 35 (in Chinese)

8 Ding Hebing, Liu Yihua, Qiao Shuxiao. *Printed Circuit Information*[J], 2010(z1): 126 (in Chinese)

9 Asahina T, Ishihara H, Asoh H *et al*. *Journal of Japan Institute of Light Metals*[J], 2008, 58(8): 375

10 Kato K. *Surface Technology*[J], 1978, 6(6): 447

11 Massardier V, Ngansop A, Fabregue D *et al*. *Metallurgical and Materials Transactions A*[J], 2012, 43(7): 2225

12 Ding Xuan, Gan Yurong, Zhang Chunju *et al*. *Heat Treatment of Metals*[J], 2021, 46(8): 174 (in Chinese)

13 Wang Zhutang. *Light Alloy Fabrication Technology*[J], 2024, 52(3): 8 (in Chinese)

14 An Xiaoxue, Li Yong, Wang Fu *et al*. *Materials Reports*[J], 2018, 32(4): 1300 (in Chinese)

15 Samberger S, Weißensteiner I, Stemper L *et al*. *Acta Materialia*[J], 2023, 253: 118952

16 Cheng Haifeng, Huang Kui, Qing Liping *et al*. *Special Casting & Nonferrous Alloys*[J], 2020, 40(9): 1027 (in Chinese)

17 Zhao Jingwei, Liu Zhengshan, Cao Yiheng *et al*. *Materials Reports*[J], 2018, 32(S2): 365 (in Chinese)

18 Yang Yong, Zhang Quancheng, Tian Qingchao. *Light Alloy Processing Technology*[J], 2022, 50(1): 25 (in Chinese)

19 Popović M, Romhanji E. *Materials Science and Engineering A*[J], 2008, 492(1–2): 460

20 Su Yuangming, Zhao Yanjun, Chen Sihao *et al*. *Rare Metal Materials and Engineering*[J], 2021, 50(3): 948 (in Chinese)

21 Zhang Chao, Huang Shenghua. *Electroplating & Pollution Control*[J], 2019, 38(5): 71 (in Chinese)

不同热处理对 Al-5.6Mg 合金板材表面组织和阳极氧化膜组织的影响

江钟宇，许光明

(东北大学 材料电磁加工教育部重点实验室，辽宁 沈阳 110819)

摘　要：研究了不同中间退火热处理对 Al-5.6Mg 合金轧制薄板表面组织和阳极氧化膜组织的影响。结果表明：在中间退火过程中，用连续退火代替箱式退火，试样表面晶粒尺寸可减小约 60%，Mg 析出相（Mg_2Al_3）尺寸可减小约 67%；在晶粒尺寸、析出相和织构的共同影响下，经连续中间退火和低温稳定化退火后阳极氧化，获得了最高的光泽度。均匀的微观结构有利于减少氧化膜的不均匀溶解，获得厚度均匀、光泽度高的阳极氧化膜。

关键词：热处理；阳极氧化；Al-Mg 合金；微观结构

作者简介：江钟宇，男，1984 年生，硕士，正高级工程师，东北大学材料电磁加工教育部重点实验室，辽宁 沈阳 110819，E-mail：zhy_jiang@chinalco.com.cn